

Article

Magnesium Impregnated on NaX Zeolite Synthesized from Cogon Grass Silica for Fast Production of Fructose via Microwave-Assisted Catalytic Glucose Isomerization

Sittichai Kulawong^{1,*}, Saran Youngjan², Pongtanawat Khemthong², Narong Chanlek³, Jatuporn Wittayakun⁴ and Nattawut Osakoo^{4,5,*}

¹ Program of Chemistry, Faculty of Science and Technology, Nakhon Ratchasima Rajabhat University, Nakhon Ratchasima 30000, Thailand

² National Nanotechnology Center (NANOTEC), National Science and Technology Development Agency (NSTDA), Klong Laung, Pathumthani 12120, Thailand; saran.you@nanotec.or.th (S.Y.); pongtanawat@nanotec.or.th (P.K.)

³ Reseach Facility, Synchrotron Light Research Institute, Nakhon Ratchasima 30000, Thailand; narong@slri.or.th

⁴ School of Chemistry, Institute of Science, Suranaree University of Technology, Nakhon Ratchasima 30000, Thailand; jatuporn@sut.ac.th

⁵ Institute of Research and Development, Suranaree University of Technology, Nakhon Ratchasima 30000, Thailand

* Correspondence: sittichai.k@nrru.ac.th (S.K.); nattawut.o@g.sut.ac.th (N.O.); Tel.: +66-862-525-250 (S.K.)



Citation: Kulawong, S.; Youngjan, S.; Khemthong, P.; Chanlek, N.; Wittayakun, J.; Osakoo, N. Magnesium Impregnated on NaX Zeolite Synthesized from Cogon Grass Silica for Fast Production of Fructose via Microwave-Assisted Catalytic Glucose Isomerization. *Catalysts* **2021**, *11*, 981. <https://doi.org/10.3390/catal11080981>

Academic Editor: Franck Launay

Received: 27 June 2021

Accepted: 12 August 2021

Published: 17 August 2021

Publisher's Note: MDPI stays neutral with regard to jurisdictional claims in published maps and institutional affiliations.



Copyright: © 2021 by the authors. Licensee MDPI, Basel, Switzerland. This article is an open access article distributed under the terms and conditions of the Creative Commons Attribution (CC BY) license (<https://creativecommons.org/licenses/by/4.0/>).

Abstract: Fructose is a crucial intermediate in the production of several chemical platforms. Fructose is mainly produced from glucose isomerization either through immobilized enzymes or heterogeneous catalysts using a conventional heating source, and this is time-consuming. Thus, this work discloses a fast production of fructose via microwave-assisted catalytic glucose isomerization using Mg catalysts supported on NaX zeolite from cogon grass silica. The catalysts were prepared by the impregnation of magnesium nitrate solution and subsequently transformed into MgO on NaX by calcination. The effect of 3, 6 and 9 wt.% Mg content on NaX on the performance of glucose isomerized to fructose was tested at 90 °C for 15 min. The best catalyst was selected for studying the effect of reaction times of 5, 15, 30 and 60 min. Results from X-ray diffraction (XRD), N₂ sorption and CO₂ temperature-programmed desorption (CO₂-TPD) suggested that crystallinity, surface area and micropore volume decrease but basicity increases with Mg content. The X-ray photoelectron spectroscopy (XPS) result confirmed the presence of mixed phases of MgO and Mg₂CO₃ in all catalysts. The glucose conversion enhanced with the Mg loading but the fructose yield gave the highest value with Mg of 6 wt.%, probably due to the tuning of high active sites and surface area. The greatest fructose selectivity and yield (71.9% and 25.8%) were obtained within 15 min by microwave-assisted catalytic reaction, shorter than the reported value in the literature, indicating a suitable reaction time. Mg (6 wt.%)/NaX catalyst preserves the original catalytic performance up to three cycles, indicating that it is a promising catalyst for fructose production.

Keywords: cogon grass silica; NaX zeolite; magnesium oxide; microwave; glucose; fructose

1. Introduction

Biomass is a desired renewable resource to employ in the chemical industry for the substitution of fossil-derived resources due to growing environmental concerns. Moreover, biomass is converted through value-added chemicals and fuels [1,2]. Lignocellulosic biomass and agricultural, industrial and forest residues have been reported as some of the alternative compounds for the sustainable production of chemicals and fuels [2,3]. The main compositions of lignocellulosic materials contain many polysaccharides of glucose as the major building block. Thus, it is accepted as the most available carbon renewable source and cheap material [2]. Generally, glucose monomers have been widely used in

the food industry and medicine [2,4]. Concurrently, they can be utilized in the synthesis of fuels and value-added chemicals [5]. One of the most crucial glucose reactions in the chemical platform is the production of fructose via isomerization because fructose is an important intermediate in the production of several platform chemicals such as 5-hydroxymethylfurfural (HMF), levulinic acid (LA), lactic acid and formic acid (FA) [6].

Typically, glucose isomerization into fructose is mainly produced by employing immobilized enzymes as catalysts (D-glucose or xylose isomerase), which is a time-consuming and high-cost technique [7]. Heterogeneous catalysts using a conventional heating source (CH) have been investigated as more advantageous in terms of the economic aspect due to the shorter reaction time and capability of regenerated and recycled catalysts [8]. Although heterogeneous catalysts with CH provide a shorter reaction time than the biological method, the completed reaction still takes several hours [4,8–11]. Recently, Hirano et al. (2020) [6] have shown an interesting result on the conversion of glucose to HMF using Ni–graphene oxide hybrid catalysts using the microwave heating method (MH), as they achieved the highest yield of HMF (28.1%) within 30 min. The thermal effect of MH is the phenomenon that microwave energy is absorbed by dielectric materials such as water, solvents and zeolites and converted into heat [12,13]. When microwave radiation penetrates the dielectric materials to supply energy, heat is generated in the whole volume, and the heat is faster and more uniform than CH [14]. Moreover, solvent, good microwave absorbers such as water could be beneficial in glucose isomerization into fructose because water could contribute heat production to the catalyst upon microwave irradiation [15]. Besides, some heterogeneous catalysts (active site and/or support) act as microwave absorbers, resulting in the overheating of the surface catalyst. The consequence could increase the reaction rate [13,15,16].

Not only the heating source but also the types of active phases and supports impact on the catalytic performance of glucose isomerization into fructose [8]. Among various active phases and supports in the literature, MgO/Na zeolites are promising catalysts for glucose isomerization into fructose due to providing a large fructose yield and low leaching rate of the active phase into a liquid phase [8,17]. The basicity of MgO has displayed a crucial role in glucose isomerization into fructose via water dissociation on the MgO surface, becoming hydroxylated and negatively charged species. The consequence facilitates the contact between glucose and the catalyst surface, leading to the presence of the 1,2-enediol intermediate. Then, it is subsequently processed via an electron pair movement through the carbon skeleton to the transformation of fructose [18]. Therefore, based on the above-mentioned reason, the enlarged basicity of the MgO catalyst could beneficially enhance with great activity [10].

Moreover, zeolites provide either basic or Lewis acid properties, presenting a drastic performance for this reaction under moderate testing conditions [8,19]. Graça et al. (2018) [9] have disclosed that magnesium-impregnated NaY zeolite outperforms glucose isomerization into fructose compared to other Na zeolites (NaMOR, NaBEA, NaZSM-5 and NaFER) in terms of the larger structure selected. Consideringly, NaY zeolite is in the faujasite framework type, similar to NaX zeolite but with a lower Si/Al ratio. The lower Si/Al ratio in NaX-incorporated Mg could generate a larger basic property that could promote glucose isomerization into fructose [10,20].

In general, the synthesis of faujasite zeolites is accomplished by using several commercial silica sources including fumed silica, tetraethyl orthosilicate (TEOS) and ludox silica, and this is a cost-consuming process [19,21,22]. Alternatively, silica from renewable sources becomes more attractive due to greener and more environmentally friendly sources. Cogon grass, a weed that is plentifully available in Thailand and tropical countries, is one of the most interesting renewable bio-silica sources [23], since it interrupts the growth of economic crops and has low commercial value [23,24]. Consequently, the traditional method to eliminate cogon grass is burning it into the environment, a simple and cheap management method. However, the consequent effect currently generates a serious problem of air pollution resulting from burning residues such as toxic gases and

PM 2.5 particles [25]. Therefore, the use of cogon grass as a silica source in zeolite synthesis would be more desirable to produce renewable silica and recycle the waste, lowering the impact on the environment [23]. Concurrently, it is reported as a potential silica source for the synthesis of NaY zeolite because it has a high purity of active silica after extraction and calcination [23,24]. To the best of our knowledge, there is no report on the synthesis of NaX zeolite from cogon grass silica. Hence, it is the desired silica source for the synthesis of NaX zeolite in this work.

To correlate with the desirable concept of the more effective strategy for fructose production, the present work aims to study the effect of microwave-assisted catalytic glucose isomerization into fructose using magnesium species supported on NaX synthesized from cogon grass silica. Moreover, properties of catalysts including crystallinity, porosity, surface area, basicity and the form of active species are characterized by X-ray diffraction (XRD), N_2 sorption, CO_2 temperature-programmed desorption (CO_2 -TPD) and X-ray photoelectron spectroscopy (XPS), respectively. The effects of magnesium content and reaction time on the performance of glucose isomerization into fructose are optimized. Finally, the reusability of the best catalyst is studied.

2. Results and Discussion

2.1. Phase of Silica from Cogon Grass

The phase of bio-silica from calcined cogon grass including with and without HCl treatment is revealed in Figure S1. When treated in HCl solution, a dominant broad peak at 22° in the calcined cogon grass was observed, indicating that the major phase of silica was amorphous. In contrast, the untreated sample gave a broad peak at 22° and other peaks at 29° , 38.5° , 43.59° and 48.17° corresponding to a mixed phase between the amorphous silica and $CaCO_3$ phases [26]. The result agrees with previous reports that amorphous silica is found as a major phase in calcined cogon grass treated with acid [23,24]. Moreover, the purity of silica in the treatment with the acid sample was 99.22 ± 0.13 , but the purity when not treated with acid was around 69.56 ± 0.33 . The result suggests that the use of acid leaching in cogon grass could eliminate other contaminated contents, resulting in higher silica purity [23]. The silica yield in the acid leaching sample was 9.25 wt.%. Importantly, the high purity and existence of an amorphous phase of silica from cogon grass in the present work make it reasonable to use as a silica source for zeolite NaX synthesis due to expediently dissolving in NaOH solution, leading to the quick generation of a zeolite synthesis precursor (Na_2SiO_3) [23].

2.2. Catalyst Characterization

XRD patterns of bare NaX and magnesium supported on NaX are demonstrated in Figure 1. For the bare NaX sample, it showed peaks at the 2θ of 6.3° , 10.3° , 12.2° , 16° , 19.1° , 20.7° , 23.3° , 24.1° , 27.6° , 31.4° , 32° and 34.8° , corresponding to characteristic peaks of zeolite NaX [27]. Other impurity peaks were not detected, indicating that the pure phase of zeolite NaX was obtained by using silica from cogon grass. When loaded with magnesium, the characteristic peaks of zeolite NaX still presented their crystal structure but were reduced in intensity with the magnesium loading. The relative crystallinity of bare supports and catalysts is calculated and concluded in Table 1. The relative crystallinity of catalysts proportionally declined with the magnesium loading. The evidence aligns with the report from Graca et al. (2017) [8] that the decrease in the zeolite NaY crystallinity in catalysts is a proportion of the Mg loading. This implies that the samples adding a larger content of Mg might affect the collapse of the zeolite structure. Noticeably, the presence of the MgO or other phases in all calcined catalysts was not observed by XRD. This remark implies that the magnesium species on NaX could present in amorphous form and/or small crystalline form (less than 5 nm), undetectable by XRD [8,28]. However, the active species on the surface of NaX zeolite could be confirmed by more powerful techniques such as XPS.

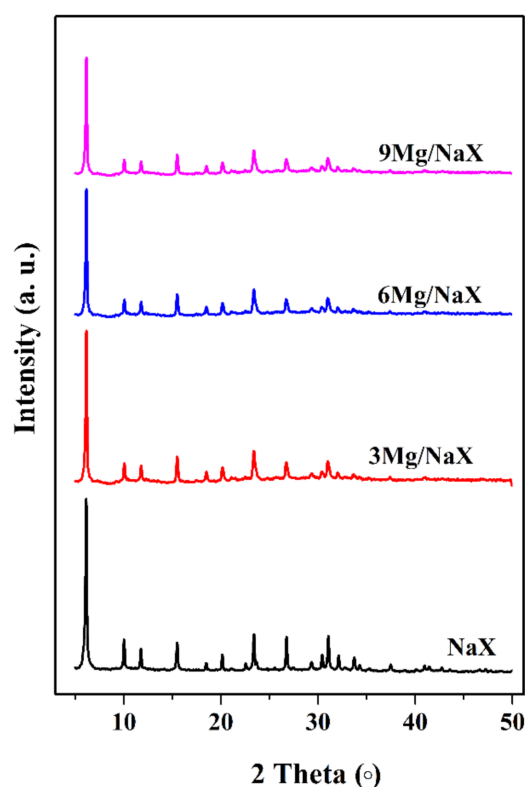


Figure 1. XRD patterns of zeolite NaX and magnesium loaded on NaX.

Table 1. Crystallinity, textural properties, basicity and magnesium content of the catalysts.

Sample	^a Crystallinity (%)	^b N ₂ -Sorption		^c CO ₂ -TPD (μmol/g)			^d Mg Content (wt.%)
		^b Surface Area (m ² g ⁻¹)	^b Micropore Volume (cm ³ g ⁻¹)	Weak	Medium	Strong	
NaX	100	630	0.27	-	241	-	-
3Mg/NaX	94.5	522	0.23	18.9	41.4	207	3.10 ± 0.08
6Mg/NaX	90.1	445	0.19	27.9	48.4	273	6.07 ± 0.02
9Mg/NaX	78.3	238	0.10	20.7	43.2	367	9.05 ± 0.03

^a Realtive crystallinity calculated according to the literature [29]. ^b Micropore, external surface areas and micropore volume obtained from t-plot method [30]. ^c Basicity determined by CO₂-TPD calculated based on the peak area compared to a reference material with a known number of basic sites [31]. ^d Mg content determined by AAS technique.

Chemical surface species of catalysts determined by XPS are demonstrated in Figure 2a,b, corresponding to Mg 2p and O 1s, respectively. The XPS result of Mg 1s (Figure 2a) consisted of two major peaks at the binding energy of 49.2 and 50.5 eV. These peaks are attributed to character positions of MgO and Mg₂CO₃ species, respectively [32]. The XPS spectra of O 1s contained three dominant peaks at 529.8, 531.4 and 532.8 eV corresponding to O–Mg, Si–O–Al in the zeolite and (CO₃)²⁻ species [21,32]. The XPS result suggests that the forms of catalyst exist in a mixed phase of MgO and Mg₂CO₃. However, it is noticeable that the peaks of Mg₂CO₃ in both Mg 2p and O 1s become stronger with Mg content, implying the larger carbonate species on the catalyst surface. This might result from the formation of greater MgO located outside the micropore, rapidly and strongly adsorbing CO₂ in the atmosphere [9].

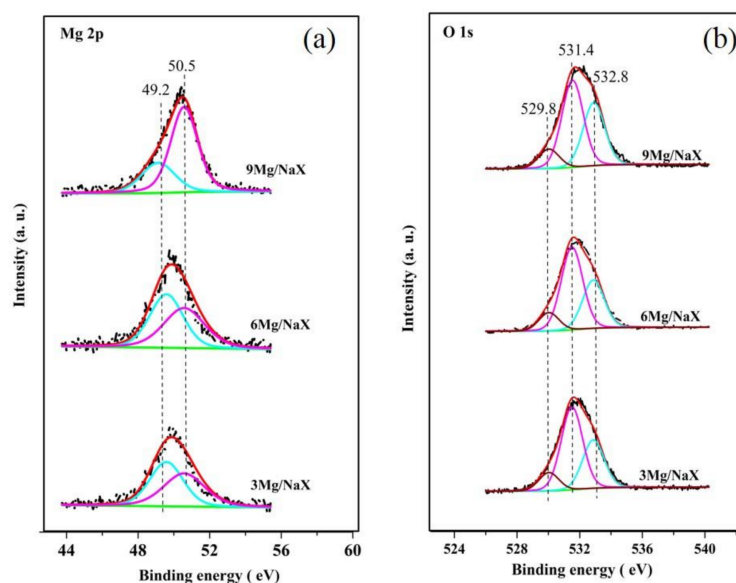


Figure 2. XPS spectra of catalysts with various magnesium contents corresponding to Mg 2p (a) and O 1s (b).

N_2 sorption isotherms of bare NaX and catalysts to evaluate the textural properties are illustrated in Figure 3. The N_2 adsorption–desorption isotherms of bare NaX showed a fast adsorbed volume of a monolayer at low relative pressure attributed to type I adsorption according to the IUPAC classification. This is typical adsorption behavior for microporous materials such as zeolites [21–23]. Remarkably, a type-H4 hysteresis loop was observed at relative pressure from 0.6–1.0 in all samples. The hysteresis loop from 0.6 to 0.85 is referred to as the filling of uniform slit-shaped intercrystal mesopores, which occur from the packing of small or nano NaX particles. Another uptake range is from a higher relative pressure, 0.85–1.0, corresponding to the filling of the macropore character generated by the packing of aggregated zeolite particles [33].

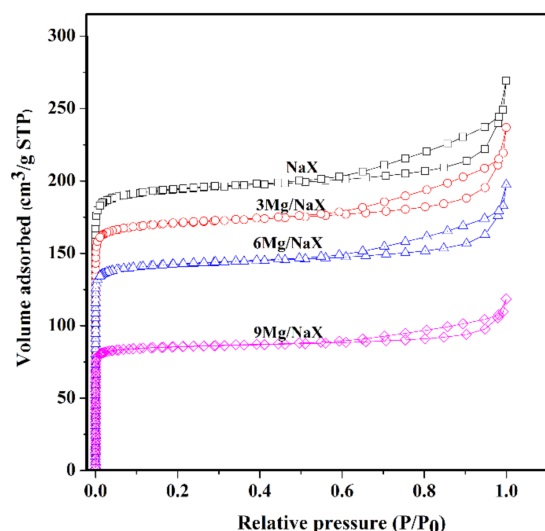


Figure 3. N_2 sorption isotherms of bare NaX and catalysts with various magnesium contents.

Noticeably, the volume adsorbed significantly decreased with the magnesium content, indicating that the magnesium species could occupy and locate throughout both micropores and mesopores, respectively [34]. The assumption agrees well with the reduction in surface area and micropore volumes displayed in Table 1. However, the drastic falls in the volume adsorbed, surface area and micropore volumes in the 9Mg/NaX catalyst were observed

probably due to the extended pore blockage of the micropores of the zeolite resulting from a large amount of Mg loading. This hypothesis correlates well with the report from Graca et al. (2017) [8] that a Mg content of 10 wt.% loaded on NaY zeolite results in an increase in the Mg species size or the partial pore blockage, resulting in a significant drop in the micropore volume and surface area.

The basicity of bare NaX and catalysts determined by CO₂-TPD is shown in Figure 4. In general, the CO₂ desorption ranges from CO₂-TPD are classified in various basic strengths, including weak basic site (50–175 °C), medium basic site (175–400 °C) and strong basic site (>400 °C) [35]. The bare NaX gave one broad peak at 322 °C, contributing to the medium basic site. The result agrees well with the report of Han et al. (2016) [36] that the basic strength of NaX zeolite provides a medium character of the basic site. This evidence is another support, implying that the synthesis of NaX zeolite from cogon grass silica is successful, consistent with the XRD result. Moreover, the basic strength of NaX zeolite is larger than that of NaY zeolite reported in the literature [8]. This could be the consequence of the greater Al content in the framework zeolite, resulting in more negatively charged oxygens possessing essential basicity and/or nucleophilicity [37].

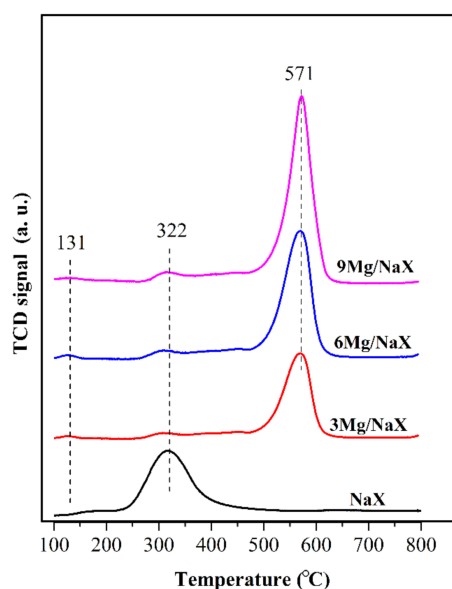


Figure 4. CO₂-TPD profiles of bare NaX and catalysts with various magnesium contents.

When loading Mg species on NaX, the desorption peaks of CO₂ were observed in three ranges: small peaks at 131 and 322 °C and a dominant peak at 571 °C corresponded to weak, medium and strong basic sites, respectively. The desorption patterns of basic sites correlate well with those of MgO species reported in the literature at 107, 286 and 545 °C attributed to the CO₂ adsorption at the position of surface hydroxyl groups, oxygen in Mg²⁺ and O²⁻ and low coordinate oxide sites that strongly interact with CO₂ in the form of bidentate carbonate and/or monodentate carbonates [8,35,38]. However, the desorption temperature of CO₂ in all catalysts was higher than that in the bare MgO reported in the literature [35], probably due to the incorporation between MgO and NaX zeolite. Besides, it is remarkable that the peak intensity at a strong basic site became more progressive with the Mg content, suggesting the presence of larger basicity [39]. This remark agrees well with the basicity amount summarized in Table 1.

2.3. Catalytic Performance of Microwave-Assisted Glucose Isomerization into Fructose

The different Mg contents incorporated into NaX zeolite impact various properties of the catalysts, such as the form of the active site, porosity and basicity including basic density and strength. Such distinguished properties in catalysts mentioned above could result in their catalytic performance. The effect of Mg content on glucose conversion,

fructose selectivity and yield is demonstrated in Figure 5. The Mg content impregnated on NaX zeolite analyzed by AAS was consistent with the calculation values, as summarized in Table 1. Noticeably, the bare NaX was also active for glucose isomerization into fructose with the highest selectivity but provided the lowest in conversion and yield. As mentioned above, the bare NaX gave a high surface area and medium basic site that could promote the reaction. This result is in good agreement with the report of Moreau and coworkers (2000) [20] that the largest fructose selectivity ($\sim 86\%$) is obtained from the bare NaX tested by the CH method. This confirms the shape and size selectivity of the NaX zeolite [8,20].

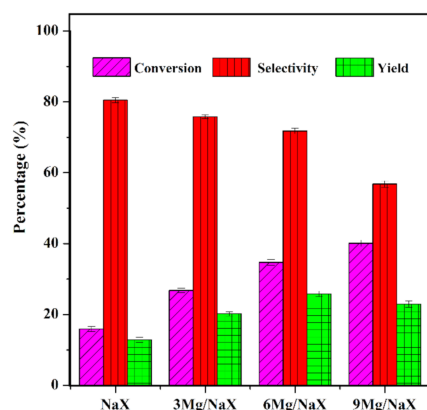


Figure 5. Effect of Mg loading catalytic performance of microwave-assisted glucose isomerization into fructose at 90 °C for 15 min with the triplicate-repeated reaction.

When adding Mg in various amounts, the glucose conversion increased with the Mg content, but the selectivity had an inverse tendency. Moreover, the fructose yield enlarged with the Mg content and reached the maximum value at the loading of 6 wt.%, but it slightly fell with the loading of 9 wt.%. The result confirms that the impregnated Mg on NaX zeolite leads to a drastic improvement in the catalyst performance according to the increase in active sites, namely, the density of basic sites [8]. However, the Mg loading of 9 wt.% could further enhance in terms of catalyst performance and the greatest conversion, but it could lower the fructose yield and selectivity. This is not very surprising because two contrasting effects could result in catalytic performance. For the first reason, the larger amounts of Mg improve the basicity of the catalysts, facilitating the activity for glucose isomerization into fructose. In another way, with the increase in Mg content, the size of the MgO species could essentially be agglomerated and/or enlarged, lowering the surface area due to the pore blockage of zeolite [8,17]. In addition, a significant drop in the crystallinity of the NaX zeolite was observed with the Mg loading of 9 wt.%, which might affect the activity by altering the dispersion and interaction of the active phase with the support.

Additionally, as mentioned earlier, the basicity of MgO exhibits a crucial role in glucose isomerization into fructose by facilitating the contact between glucose and the catalyst surface, generating the 1,2-enediol intermediate followed subsequently by the production of fructose via an electron pair movement through the carbon skeleton [18]. However, one should note that glucose isomerization is a reversible reaction in that the maximum glucose conversion to fructose could be thermodynamically limited. Consequently, the overload basicity of the catalyst could promote the production of by-products and improve glucose conversion, but it could lower the fructose yield [10]. Hence, based on the reasons above, 6Mg/NaX with the greatest fructose yield and high selectivity is selected as the best catalyst in the present study, probably due to the tuning of high basic sites and surface area and the further optimization of reaction time.

The effect of reaction times including 5, 15, 30 and 60 min for the performance of glucose isomerization into fructose on the 6Mg/NaX catalyst is revealed in Figure 6. It was noticed that the glucose conversion improved sharply from the reaction time of 5 to 15 min and slightly increased when prolonged to 30 and 60 min, respectively. The evidence

suggests that the reaction rate is likely very fast by using the MH method and reaches almost steady conversion within 15 min. Such catalytic behavior correlates well with the report from Lecomate et al. (2002) [40] that the glucose conversion of KX zeolite catalyst tested by the CH method slightly enhanced from 60 to 90 min, but became constant after the reaction time of 120 min. The faster reaction rate in glucose isomerization to fructose by MH could result from the overheating of the surface catalyst generated by the dielectric property of the solid catalyst absorbing microwave radiation [13,15]. This remark may be possible because NaX zeolite contains the defect sites of the hydroxyl (-OH) group, with the dielectric property acting as a microwave absorber serving heat to promote the adjacent Mg species [41]. This assumption agrees well with the report of Yu and coworkers (2019) [15] that oxygen-containing groups on pristine GIO/GO including carboxyl, hydroxyl and epoxy groups acting as microwave absorbers could be conducive to generate microwave-active Al active sites for glucose isomerization to fructose. The result leads to a fructose yield of 34% with a reaction time of 20 min, compared to CH with a fructose yield of 2% and at a similar reaction time. This evidence suggests that the application of the MH method instead of the CH method essentially promotes a faster reaction rate. However, fructose yield and selectivity achieved the highest values with the reaction time of 15 min and then dramatically dropped with the extended reaction time of 30 and 60 min, along with a small increase in glucose conversion, respectively. This is certainly evidence that the by-products, probably mannose and HMF (seen in Figure S2 in Supplementary Materials), are generated from the further transformation of fructose, as suggested by Graca et al. (2017) and Marianou et al. (2018) [8,10]. Additionally, Xiouras et al. (2016) [42] suggested that prolonged residence times from 10 min to 15 min of microwave-assisted catalytic xylose to furfural in a homogeneous catalyst of NaCl (5 wt.%) decrease the yield of furfural because this may promote a side reaction. Similarly, Hirano et al. (2020) [6] have recently found that a high fructose yield and selectivity are observed in the reaction time of around 10–15 min on Ni–graphene oxide hybrid catalysts in the production of HMF by the MH method. Therefore, the suitable time for glucose isomerization into fructose in the present work is 15 min due to providing the highest fructose yield and moderate selectivity. On the other hand, one should note that the largest fructose yield in 6Mg/NaX at the reaction time of 15 min may cause the effect of resonant microwave fields in liquid phase batch processing in vessels. The result could provide non-uniform heat in space and time [43,44]. Consequently, the temperature of the liquid phase inside the vessel at 15 min might be higher than that at other varied times. The observation is in good agreement with several reports in the literature [43–45]. However, this effect should be studied in more detail in terms of the heterogeneous catalyst in future work.

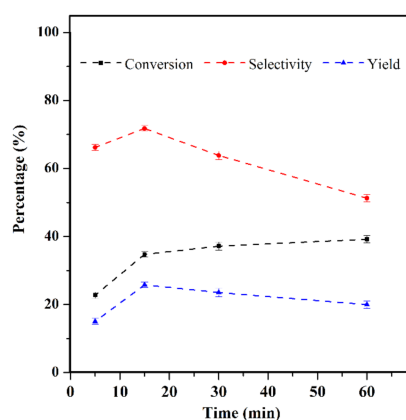


Figure 6. Effect of reaction time in the catalytic performance of microwave-assisted glucose isomerization into fructose on 6Mg/NaX catalyst at 90 °C with the triplicate-repeated reaction.

2.4. Catalyst Regeneration and Reuse

Regeneration and reuse catalysts are also important factors correlating the more cost-effective of catalytic testing processes. Accordingly, Graca et al. (2017) [8] have suggested that fructose yield and selectivity on the reuse of 5% MgNaY zeolite combined with catalyst regeneration give much greater than that without catalyst regeneration due to the removal of carbonaceous species (coke) deposited on the catalyst and zeolite surface.

Thus, the 6Mg/NaX catalyst was regenerated by calcination in air for 1 h before use in each cycle, as demonstrated in Figure 7. The glucose conversion and fructose yield and selectivity could nearly preserve the original activity of the first run; the conversion and yield slightly declined with the number of reaction cycles, up to the third cycle, but the fructose selectivity gradually improved. There are several factors that could lead to the presence of such behavior in catalyst reusability: (i) magnesium species might gradually leach into the liquid phase in each consecutive run, causing a decrease in basicity; (ii) the agglomeration of magnesium particles might occur during each calcination step in catalyst regeneration; and (iii) partial collapse of the zeolite structure during each regeneration cycle might occur due to calcination at a high temperature (600 °C for 1 h) resulting in changes in catalyst interaction and dispersion [8,46]. Importantly, it was noticed that significant drops in the conversion, yield and selectivity were observed in the fourth run. The assumptions seem consistent with the presence of a trace amount of Mg leaching into the liquid phase in each cycle run, as demonstrated in Table S2 in Supplementary Materials. In addition, the XRD intensity and relative crystallinity of NaX zeolite from the spent catalyst in the fourth run were dramatically poor, mostly structure-damaged, compared with the other cycles (as shown in Figure S2 in Supplementary Materials). This evidence may suggest that the deactivation of the catalyst in the present study is mainly from the overextended collapse of the NaX zeolite structure. Noticeably, the gradual partial collapse of the zeolite structure seems beneficial for the fructose selectivity, as presented in the gradual increase in the percentage of selectivity from the first run to the third run. Therefore, the result suggests that Mg (6 wt.%) impregnated on NaX zeolite synthesized from cogon grass silica has high stability up to three cycles, and that it could be a useful and promising catalyst for glucose isomerization into fructose.

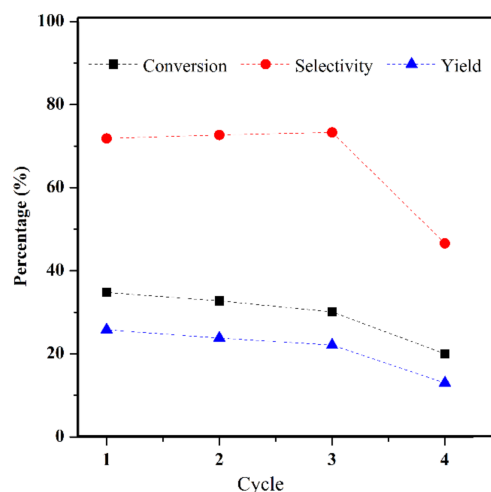


Figure 7. Regeneration and reuse catalyst in the catalytic performance of microwave-assisted glucose isomerization into fructose on 6Mg/NaX catalyst at 90 °C for 15 min.

2.5. Comparison of Catalytic Performances of the Best Catalyst in the Present Work to the Relevant Literature

Compared to other relevant literature, based on the determination of fructose yield, productivity and reaction time, the catalyst in the present work provided the highest fructose productivity rate ($(\text{g}_{\text{fructose}}/\text{g}_{\text{catalyst}}/\text{h})$) with a shorter reaction time, as shown in Table 2. Thus, an improvement in the performance of fructose production via microwave-

assisted catalytic glucose isomerization using magnesium impregnated on NaX from cogon grass (6Mg/NaX) was accomplished. Moreover, a renewable bio-silica source, namely, cogon grass, was used as the silica source for NaX zeolite synthesis, which is another advantage to the environment. Overall, this suggests that 6Mg/NaX catalysts in the present work could be considered promising catalysts for glucose isomerization into fructose, especially in terms of fast fructose production with an environmentally friendly strategy.

Table 2. Comparison of glucose conversion, fructose yield and selectivity using microwave-assisted catalytic glucose isomerization in the present work to relevant literature.

Catalyst	Temp. (°C)	Time (h)	Catalyst Amount (g)	Fructose Yield (%)	Fructose Productivity (g fructose/g catalyst/h)	Ref.
NaX	95	1	1	17	0.57	[20]
Hydrotalcite (Mg/Al = 2.5)	95	1	1	20	0.84	[20]
10% MgNaY	100	0.5	0.1	31	6.20	[8]
Fe/beta-zeolite (0.060)	150	1.5	0.1	22	1.46	[11]
Natural-MgO	90	0.75	1	33.4	3.56	[10]
Sodium titanate nanotubes	90	0.5	0.15	30.8	6.41	[42]
NaX from cogon grass	90	0.25	0.15	12.5	3.22	This work
6Mg/NaX from cogon grass	90	0.25	0.15	25.8	6.88	This work

3. Materials and Methods

3.1. Silica Production from Cogon Grass

Silica from cogon grass was obtained by acid leaching the dried cogon grass from a method modified from the work of Bunmai et al. (2018) and Kulawong et al. (2018) [23,24]. Shortly, dried cogon grass was cut into small pieces (1–3 cm), cleaned with deionized water (DI) and dried at 90 °C for 120 h. Afterward, the dried grass (30.5 g) was treated in 400 mL of hydrochloric acid (37% HCl, Carlo Erba, CARLO ERBA Reagents S.A.S., Chau. du Vexin, France) solution (2.0 M) in a round bottom flask of 1000 mL size connected with a condenser at 90 °C for 3 h. Then, the treated grass was separated by filtration and subsequently washed with DI several times. Then, it was kept at room temperature for one day and calcined at 550 °C for 6 h. Finally, silica powder was obtained and the yield was quantified following Equation (1) [23].

$$\text{Yield of silica powder} = \frac{\text{weight of calcined cogon grass}}{\text{weight of dried cogon grass}} \times 100 \quad (1)$$

Importantly, the extraction procedure was repeated many times to obtain an adequate silica content for zeolite synthesis.

3.2. Synthesis of NaX Zeolite

The synthesis of NaX zeolite was performed following a method adapted from Jantarit et al. (2020) [27]. The gel of NaX zeolite with the molar composition of NaAlO₂: 4SiO₂: 16NaOH: 325H₂O was prepared. Firstly, sodium silicate solution (14.68 g) was prepared by slowly dissolving silica (SiO₂) from cogon grass (4.17 g) in a solution of sodium hydroxide (97% NaOH, Carlo Erba, CARLO ERBA Reagents S.A.S., Chau. du Vexin, France) prepared from a NaOH pellet (1.65 g) and DI water (8.98 g) in a 250 mL polypropylene bottle and stirred for 20 h. Then, in another 250 mL polypropylene bottle, sodium aluminate (95% NaAlO₂, Riedel-de Haën®, Honeywell, Seelze, Germany) solution (98.46 g) was obtained by mixing a sodium hydroxide pellet (9.08 g) and NaAlO₂ (1.38 g) into DI water (88.3 g), and this was stirred for 30 min. Then, the two solutions were immediately mixed and continuously stirred for 2 h. Subsequently, the gel mixture was crystallized at 90 °C for 20 h. Then, the solid product was obtained by filtration, cleaned with DI water and dried at 90 °C for 24 h to obtain NaX as the catalyst support.

3.3. Catalyst Preparation

$x\text{Mg}/\text{NaX}$ ($x = 3, 6$ and 9 wt.%) catalysts were prepared by incipient wetness impregnation with a magnesium solution of magnesium nitrate hexahydrate precursor (99% $\text{Mg}(\text{NO}_3)_2 \cdot 6\text{H}_2\text{O}$, Sigma-Aldrich, St. Louis, Missouri, USA). Then, the mixture was further treated by ultrasonication (Ultrasonic Cleaner, ELMA-E30H, Advance Metrology Co., Ltd., Pathumthani, Thailand) using a frequency of 28 kHz and power of 100 W at 30 °C for 10 min modified from the literature [31]. Afterward, the samples were dried at room temperature for 24 h and 100 °C in an oven overnight and subsequently calcined at 500 °C in the air for 3 h. Finally, samples were named according to the magnesium loading: 3Mg/NaX, 6Mg/NaX and 9Mg/NaX, respectively.

3.4. Characterization of Cogon Grass Silica and Catalyst

The phases of NaX and Mg dispersed on NaX were determined by XRD (a Bruker, D8 Advance, Bruker Corporation, Massachusetts, USA) using $\text{Cu K}\alpha$ radiation. The current and potential during the measurement were applied at 40 mA and 40 kV [23]. Their surface area and pore volumes were analyzed by nitrogen adsorption–desorption analysis (a BELSORP-max) at -196 °C. Before analysis, the degassed sample was applied under a vacuum at 300 °C for 24 h. The t -plot method was employed to evaluate the surface area and micropore volume [30]. The basicity of catalysts was studied by CO_2 -TPD on Quantachrome; ChemBET™ Pulsar. The active species of the surface catalyst was determined by XPS (ULVAC-PHI, PHI 500 VersaProbe II, ULVAC-PHI, Inc. Japan) using Al $\text{K}\alpha$ radiation. Each sample was dried at 90 °C for 24 h to remove physisorbed water and then dispersed on carbon tape. During the measurement, the vacuum at lower than 10^{-9} mbar was applied in the chamber. A reference spectrum was the C1s photoelectron line at 284.80 eV. Silica and Mg contents supported on NaX zeolite were detected by using atomic absorption spectroscopy (AAS, Flame, Varian-55B, Varian, Inc., Palo Alto, CA, USA according to the method adapted in the literature [23].

3.5. Catalytic Testing for Glucose Isomerization into Fructose

Microwave-assisted catalytic glucose isomerization was tested by employing a microwave digestion system (Speedwave Xpert, Berghof Products, Eningen, Germany) in 40.0 mL of a vessel lined with Teflon (X press Plus, Berghof Products, Eningen, Germany) [24]. Before reaction testing, a solution consisting of 0.5 g of D-glucose ($\geq 99.5\%$ $\text{C}_6\text{H}_{12}\text{O}_6$, Sigma-Aldrich, St. Louis, MO, USA) in 10 mL of DI water was prepared and poured into the Teflon vessel, and already added to the catalyst of 150 mg. Then, nitrogen gas was purged in the Teflon vessel, which was immediately sealed to avoid air entering the system. Then, the microwave-assisted catalytic reaction was tested by using a dual microwave system with two unpulsed regulated magnetrons with a frequency of 2.45 GHz and providing a maximum power of 2000 W. The desired reaction temperature was set at 90 °C for various times including 5, 15, 30, 60 min, respectively. Time zero of the reaction was recorded when the reaction temperature reached its set point of 90 °C. The pressure inside the vessel at 90 °C was 3 bar, detected by a contactless optical sensor in real-time. Moreover, the temperature inside the vessel during catalytic testing was monitored by a patented temperature monitoring system of Speedwave direct infrared control (DIRC). This system physically determines the temperature radiation emitted by the vessel contents, the reactant solution. Radiation components emitted by the vessel walls and, in particular, the exterior of the vessel, were completely filtered out. Therefore, the system determines the temperature inside the pressure vessels by measuring the direct infrared radiation emitted by the sample. This information is forwarded to the power control module, which uses the highest measured temperature to regulate the oven power. Continuous adjustment of the magnetron output allows the temperature to be regulated on the basis of all vessel contents (seen in Figure 8) [47]. The actual temperature of each sample was displayed on the screen in real-time, 90 ± 3.0 °C, respectively.

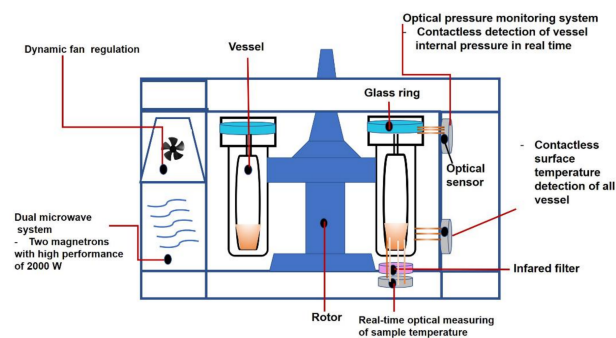


Figure 8. Microwave details of a microwave digestion system (Speedwave Xpert, Berghof Products, Eningen, Germany) adapted from a manual of Speedwave Xpert microwave [47].

After the reaction, the solution was cooled down to room temperature. Then, the liquid product and catalyst were separated by centrifugation at 3500 rpm for 10 min. Subsequently, each liquid sample was diluted in water and determined by high-performance liquid chromatography (HPLC) using a Hitachi system equipped with a refractive index detector (RID) to quantify glucose conversion, fructose yield and selectivity. The analysis was carried out with VertiSep™ SUGAR CMP HPLC column (7.8 × 300 mm internal diameter, 9 μm particle size (Vertical Chromatography Co. Ltd, Nonthaburi, Thailand) as a guard column. The temperature column was set at 80 °C throughout the analysis. In addition, the mobile phase employed in the analysis was H₃PO₄ aqueous solution (0.1% (v/v)) with a flow rate of 0.6 mL/min. Conversion of glucose, yield and selectivity of fructose were evaluated based on Equations (2)–(4), respectively.

$$\text{Conversion (\%)} = \frac{\text{mole of glucose}_{\text{input}} - \text{mole of glucose}_{\text{detected}}}{\text{mole of glucose}_{\text{input}}} \times 100 \quad (2)$$

$$\text{Selectivity (\%)} = \frac{\text{mole of fructose}_{\text{produced}}}{\text{mole of glucose}_{\text{input}} - \text{mole of glucose}_{\text{detected}}} \times 100 \quad (3)$$

$$\text{Yield (\%)} = \frac{\text{mole of fructose}_{\text{produced}}}{\text{mole of glucose}_{\text{input}}} \quad (4)$$

3.6. Regeneration and Reuse Catalyst

The best catalyst was selected for further study of regeneration and reusability by four testing cycles. After each cycle of catalytic testing, the catalyst was separated by centrifugation at 3500 rpm for 10 min and dried at 100 °C in an oven overnight and subsequently calcined at 600 °C in the air for 1 h [9]. Then, the calcined sample was further used for a second run for glucose isomerization at 90 °C for 15 min by the microwave-assisted reaction method. Additionally, the reused catalyst was applied with a similar process mentioned above for the third and fourth cycles, respectively.

4. Conclusions

This is the first report on NaX zeolite from cogon grass silica, which was successfully synthesized and used as a catalyst support for magnesium (Mg) species in the fast production of fructose via microwave-assisted catalytic glucose isomerization. The influences of Mg contents of 3, 6 and 9 wt.% on NaX, reaction time and the reusability of the best catalyst on the performance of glucose isomerized to fructose were intensively studied. All catalysts were prepared by the impregnation of magnesium nitrate solution combined with sonication and subsequently transformed to MgO on NaX by calcination at 500 °C for 3 h. Then, the physicochemical properties of catalysts were characterized by XRD, N₂ sorption, XPS and CO₂-TPD. Results from characterizations indicated that crystallinity, surface area and micropore volume reduced with the Mg content, but basicity increased. The active

species in all catalysts presented in the form of mixed phases of MgO and Mg₂CO₃. After reaction testing on glucose isomerization into fructose at 90 °C for 15 min, the glucose conversion improved with the Mg loading, but the fructose yield reached the maximum value with the loading of 6 wt.%, probably due to the tuning of high active sites and surface area. In addition, the use of microwave-assisted catalytic glucose isomerization in 6Mg/NaX catalysts provided the greatest fructose yield of 25.8% with a shorter reaction time of 15 min as well as better fructose productivity than the reported value in the literature. The reusability of the catalyst preserves the original catalytic performance up to three cycles, indicating that it is a promising catalyst for glucose isomerization to fructose.

Supplementary Materials: The following are available online at <https://www.mdpi.com/article/10.3390/catal11080981/s1>, Figure S1: XRD patterns of calcined cogon grass with and without HCl treatment (2.0 M), Figure S2: HPLC chromatogram of the products obtained from 9Mg/NaX catalyst, Figure S3: XRD patterns of spent 6Mg/NaX catalyst with each consecutive run, Table S1: Solid yield after calcination based on the weight of dried cogon grass and chemical composition determined by AAS, Table S2: Relative crystallinity and Mg leaching content of consecutive cycle runs.

Author Contributions: Conceptualization, S.K. and N.O.; methodology, S.K.; software, S.K.; validation, S.K., N.O. and J.W.; formal analysis, S.Y., N.C. and P.K.; investigation, S.K. and S.Y.; resources, P.K.; data curation, S.K. and N.O.; writing—original draft preparation, S.K. and N.O.; writing—review and editing, S.K. and N.O.; visualization, S.K. and N.O.; supervision, N.O., P.K. and J.W.; project administration, S.K.; funding acquisition, S.K. All authors have read and agreed to the published version of the manuscript.

Funding: This research received no external funding.

Data Availability Statement: Data are contained within the article.

Acknowledgments: The authors acknowledge support from the Program of Chemistry, Faculty of Science and Technology (Nakhon Ratchasima Rajabhat University, Nakhon Ratchasima, Thailand) for the experimental equipment facility and the SUT-NANOTEC-SLRI Beamline 5.3 (Synchrotron Light Research Institute, Thailand) for XPS measurement. Also, Full-Time Doctoral Researcher Grants for Osakoo, N is supported by Suranaree University of Technology (SUT) and by Thailand Science Research and Innovation (TSRI).

Conflicts of Interest: The authors declare no conflict of interest.

References

1. Huber, G.W.; Iborra, S.; Corma, A. Synthesis of transportation fuels from biomass: Chemistry, catalysts, and engineering. *Chem. Rev.* **2006**, *106*, 4044–4098. [[CrossRef](#)]
2. Maity, S.K. Opportunities, recent trends and challenges of integrated biorefinery: Part I, *Renew. Sustain. Energy Rev.* **2015**, *43*, 1427–1445. [[CrossRef](#)]
3. Mohan, D.; Pittman, C.U., Jr.; Steele, P.H. Pyrolysis of wood/biomass for bio-oil: A critical review. *Energy Fuels* **2006**, *20*, 848–889. [[CrossRef](#)]
4. Graça, I.; Bacariza, M.C.; Chadwick, D. Glucose isomerisation into fructose over Mg-impregnated Na-zeolites: Influence of zeolite structure. *Microporous Mesoporous Mater.* **2018**, *255*, 130–139. [[CrossRef](#)]
5. Chheda, J.N.; Huber, G.W.; Dumesic, J.A. Liquid-phase catalytic processing of biomass-derived oxygenated hydrocarbons to fuels and chemicals. *Angew. Chem. Int. Ed.* **2007**, *46*, 7164–7183. [[CrossRef](#)] [[PubMed](#)]
6. Hirano, Y.; Beltramini, J.N.; Mori, A.; Nakamura, M.; Karim, M.R.; Kim, Y.; Nakamura, M.; Hayami, S. Microwave-assisted catalytic conversion of glucose to 5-hydroxymethylfurfural using “three dimensional” graphene oxide hybrid catalysts. *R. Soc. Chem. Adv.* **2020**, *10*, 11727–11736. [[CrossRef](#)]
7. Buchholz, K.; Seibel, J. Industrial carbohydrate biotransformations. *Carbohydr. Res.* **2008**, *343*, 1966–1979. [[CrossRef](#)]
8. Graça, I.; Iruretagoyena, D.; Chadwick, D. Glucose isomerisation into fructose over magnesium-impregnated NaY zeolite catalysts. *Appl. Catal. B Environ.* **2017**, *206*, 434–443. [[CrossRef](#)]
9. Graça, I.; Bacariza, M.C.; Fernandes, A.; Chadwick, D. Desilicated NaY zeolites impregnated with magnesium as catalysts for glucose isomerisation into fructose. *Appl. Catal. B Environ.* **2018**, *224*, 660–670. [[CrossRef](#)]
10. Marianou, A.A.; Michailof, C.M.; Ipsakis, D.K.; Karakoulia, S.A.; Kalogiannis, K.G.; Yiannoulakis, H.; Triantafyllidis, K.S.; Lappas, A.A. Isomerization of glucose into fructose over natural and synthetic MgO catalysts. *ACS Sustain. Chem. Eng.* **2018**, *6*, 16459–16470. [[CrossRef](#)]

11. Xu, S.; Zhang, L.; Xiao, K.; Xia, H. Isomerization of glucose into fructose by environmentally friendly Fe/ β zeolite catalysts. *Carbohydr. Res.* **2017**, *446–447*, 48–51. [[CrossRef](#)] [[PubMed](#)]
12. Nagahata, R.; Takeuchi, K. Encouragements for the Use of Microwaves in Industrial Chemistry. *Chem. Rec.* **2019**, *19*, 51–64. [[CrossRef](#)]
13. Palma, V.; Barba, D.; Cortese, M.; Martino, M.; Renda, S.; Meloni, E. Microwaves and heterogeneous catalysis: A review on selected catalytic processes. *Catalysts* **2020**, *10*, 246. [[CrossRef](#)]
14. Gude, V.G.; Patil, P.; Deng, S. Microwave energy potential for large scale biodiesel production. In Proceedings of the World Renewable Energy Forum, WREF 2012, Including World Renewable Energy Congress XII and Colorado Renewable Energy Society (CRES) Annual Conference, Denver, CO, USA, 13–17 May 2012; pp. 751–759.
15. Iris, K.M.Y.; Xiong, X.; Tsang, D.C.W.; Ng, Y.H.; Clark, J.H.; Fan, J.; Zhang, S.; Hu, C.; Ok, Y.S. Graphite oxide- and graphene oxide-supported catalysts for microwave-assisted glucose isomerisation in water. *Green Chem.* **2019**, *21*, 4341–4353. [[CrossRef](#)]
16. Zhang, X.; Hayward, D.O.; Mingos, D.M.P. Effects of microwave dielectric heating on heterogeneous catalysis. *Catal. Lett.* **2003**, *88*, 33–38. [[CrossRef](#)]
17. Li, B.; Li, L.W.; Dong, Y.N.; Zhang, Q.; Weng, W.Z.; Wan, H.L. Glucose isomerization into fructose catalyzed by MgO/NaY catalyst. *Chin. J. Chem. Phys.* **2018**, *31*, 203–210. [[CrossRef](#)]
18. Marianou, A.A.; Michailof, C.M.; Pineda, A.; Iliopoulou, E.F.; Triantafyllidis, K.S.; Lappas, A.A. Glucose to fructose isomerization in aqueous media over homogeneous and heterogeneous catalysts. *ChemCatChem* **2016**, *8*, 1100–1110. [[CrossRef](#)]
19. Mintova, S.; Grand, J.; Valtchev, V. Nanosized zeolites: Quo Vadis? *C. R. Chim.* **2016**, *19*, 183–191. [[CrossRef](#)]
20. Moreau, C.; Durand, R.; Roux, A.; Tichit, D. Isomerization of glucose into fructose in the presence of cation-exchanged zeolites and hydrotalcites. *Appl. Catal. A Gen.* **2000**, *193*, 257–264. [[CrossRef](#)]
21. Osakoo, N.; Pansakdanon, C.; Sosa, N.; Deekamwong, K.; Keawkumay, C.; Rongchapo, W.; Chanlek, N.; Jitcharoen, J.; Prayoonpokarach, S.; Wittayakun, J. Characterization and comprehension of zeolite NaY/mesoporous SBA-15 composite as adsorbent for paraquat. *Mater. Chem. Phys.* **2017**, *193*, 470–476. [[CrossRef](#)]
22. Sharma, P.; Jeong, S.J.; Han, M.H.; Cho, C.H. Influence of silica precursors on octahedron shaped nano NaY zeolite crystal synthesis. *J. Taiwan Inst. Chem. Eng.* **2015**, *50*, 259–265. [[CrossRef](#)]
23. Bunmai, K.; Osakoo, N.; Deekamwong, K.; Rongchapo, W.; Keawkumay, C.; Chanlek, N.; Prayoonpokarach, S.; Wittayakun, J. Extraction of silica from cogon grass and utilization for synthesis of zeolite NaY by conventional and microwave-assisted hydrothermal methods. *J. Taiwan Inst. Chem. Eng.* **2018**, *83*, 152–158. [[CrossRef](#)]
24. Kulawong, S.; Chanlek, N.; Osakoo, N. Facile synthesis of hierarchical structure of NaY zeolite using silica from cogon grass for acid blue 185 removal from water. *J. Environ. Chem. Eng.* **2020**, *8*, 104114. [[CrossRef](#)]
25. Pongpiachan, S.; Hattayanone, M.; Cao, J. Effect of agricultural waste burning season on PM_{2.5}-bound polycyclic aromatic hydrocarbon (PAH) levels in Northern Thailand. *Atmos. Pollut. Res.* **2017**, *8*, 1069–1080. [[CrossRef](#)]
26. Viriya-Empikul, N.; Krasae, P.; Nualpaeng, W.; Yoosuk, B.; Faungnawakij, K. Biodiesel production over Ca-based solid catalysts derived from industrial wastes. *Fuel* **2012**, *92*, 239–244. [[CrossRef](#)]
27. Jantarit, N.; Tayraukham, P.; Osakoo, N.; Föttinger, K.; Wittayakun, J. Formation of EMT/FAU intergrowth and nanosized SOD zeolites from synthesis gel of zeolite NaX containing ethanol. *Mater. Res. Express* **2020**, *7*, 075011. [[CrossRef](#)]
28. Osakoo, N.; Khemthong, P.; Roessner, F.; Kidkhunthod, P.; Chanlek, N.; Prayoonpokarach, S.; Wittayakun, J. Development and characterization of silica supported cobalt oxides for ethanol oxidation using different preparation methods, *Radiat. Phys. Chem.* **2020**, *171*, 108718. [[CrossRef](#)]
29. Oruji, S.; Khoshbin, R.; Karimzadeh, R. Preparation of hierarchical structure of Y zeolite with ultrasonic-assisted alkaline treatment method used in catalytic cracking of middle distillate cut: The effect of irradiation time. *Fuel Process. Technol.* **2018**, *176*, 283–295. [[CrossRef](#)]
30. Baranowski, C.J.; Bahmanpour, A.M.; Héroguel, F.; Luterbacher, J.S.; Kröcher, O. Prominent role of mesopore surface area and external acid sites for the synthesis of polyoxymethylene dimethyl ethers (OME) on a hierarchical H-ZSM-5 zeolite. *Catal. Sci. Technol.* **2019**, *9*, 366–376. [[CrossRef](#)]
31. Rakmae, S.; Osakoo, N.; Pimsuta, M.; Deekamwong, K.; Keawkumay, C.; Butburee, T.; Faungnawakij, K.; Geantet, C.; Prayoonpokarach, S.; Wittayakun, J.; et al. Defining nickel phosphides supported on sodium mordenite for hydrodeoxygenation of palm oil. *Fuel Process. Technol.* **2020**, *198*, 106236. [[CrossRef](#)]
32. Chen, J.L.; Zhu, J.H. A query on the Mg 2p binding energy of MgO. *Res. Chem. Intermed.* **2019**, *45*, 947–950. [[CrossRef](#)]
33. Huang, Y.; Wang, K.; Dong, D.; Li, D.; Hill, M.R.; Hill, A.J.; Wang, H. Synthesis of hierarchical porous zeolite NaY particles with controllable particle sizes. *Microporous Mesoporous Mater.* **2010**, *127*, 167–175. [[CrossRef](#)]
34. Manadee, S.; Sophiphun, O.; Osakoo, N.; Supamathanon, N.; Kidkhunthod, P.; Chanlek, N.; Wittayakun, J.; Prayoonpokarach, S. Identification of potassium phase in catalysts supported on zeolite NaX and performance in transesterification of Jatropha seed oil. *Fuel Process. Technol.* **2017**, *156*, 62–67. [[CrossRef](#)]
35. Selvamani, T.; Sinhamahapatra, A.; Bhattacharjya, D.; Mukhopadhyay, I. Rectangular MgO microsheets with strong catalytic activity. *Mater. Chem. Phys.* **2011**, *129*, 853–861. [[CrossRef](#)]
36. Han, H.; Liu, M.; Ding, F.; Wang, Y.; Guo, X.; Song, C. Effects of cesium ions and cesium oxide in side-chain alkylation of toluene with methanol over cesium-modified zeolite X. *Ind. Eng. Chem. Res.* **2016**, *55*, 1849–1858. [[CrossRef](#)]
37. Busca, G. Acidity and basicity of zeolites: A fundamental approach. *Microporous Mesoporous Mater.* **2017**, *254*, 3–16. [[CrossRef](#)]

38. Hu, J.; Zhu, K.; Chen, L.; Kübel, C.; Richards, R. MgO(111) Nanosheets with unusual surface activity. *J. Phys. Chem. C* **2007**, *111*, 12038–12044. [[CrossRef](#)]
39. Arishtirova, K.; Kovacheva, P.; Vassilev, S. BaO/NaX zeolite as a basic catalyst for oxidative methylation of toluene with methane. *Appl. Catal. A Gen.* **2001**, *213*, 197–202. [[CrossRef](#)]
40. Lecomte, J.; Finiels, A.; Moreau, C. Kinetic study of the isomerization of glucose into fructose in the presence of anion-modified hydrotalcites. *Starch Staerke* **2002**, *54*, 75–79. [[CrossRef](#)]
41. Turner, M.D.; Laurence, R.L.; Conner, W.C.; Yngvesson, K.S. Microwave radiation's influence on sorption and competitive sorption in zeolites. *Am. Inst. Chem. Eng. J.* **2000**, *46*, 758–768. [[CrossRef](#)]
42. Xiouras, C.; Radacsi, N.; Sturm, G.; Stefanidis, G.D. Furfural synthesis from D-xylose in the presence of sodium chloride: Microwave versus conventional heating. *ChemSusChem* **2016**, *9*, 2159–2166. [[CrossRef](#)] [[PubMed](#)]
43. Sturm, G.S.J.; Verweij, M.D.; Van Gerven, T.; Stankiewicz, A.I.; Stefanidis, G.D. On the effect of resonant microwave fields on temperature distribution in time and space. *Int. J. Heat Mass Transf.* **2012**, *55*, 3800–3811. [[CrossRef](#)]
44. Sturm, G.S.J.; Verweij, M.D.; Van Gerven, T.; Stankiewicz, A.I.; Stefanidis, G.D. On the parametric sensitivity of heat generation by resonant microwave fields in process fluids. *Int. J. Heat Mass Transf.* **2013**, *57*, 375–388. [[CrossRef](#)]
45. Cherbański, R.; Rudniak, L. Modelling of microwave heating of water in a monomode applicator e Influence of operating conditions. *Int. J. Therm. Sci.* **2013**, *74*, 214–229. [[CrossRef](#)]
46. Kumar, S.; Nepak, D.; Kansal, S.K.; Elumalai, S. Expeditious isomerization of glucose to fructose in aqueous media over sodium titanate nanotubes. *R. Soc. Chem. Adv.* **2018**, *8*, 30106–30114. [[CrossRef](#)]
47. Manual User, Speedwave Xpert Microwave Digestion System. Available online: <https://www.berghof-instruments.com/en/product/speedwave-xpert> (accessed on 2 August 2021).